Vol.65: e22200784, 2022
https://doi.org/10.1590/1678-4324-2022200784
ISSN 1678-4324 Online Edition

Article - Human and Animal Health

Synthesis and in Vitro Toxicity Assessment of Different Nano-Calcium Phosphate Nanoparticles

Toğar Başak[1*]
https://orcid.org/0000-0003-0883-0458

Türkez Hasan[2]
https://orcid.org/0000-0002-7046-8990

Bakan Feray[3]
https://orcid.org/0000-0001-6467-8943

Arslan Mehmet Enes[4]
https://orcid.org/ 0000-0002-1600-2305

Tatar Abdulgani[5]
https://orcid.org/ 0000-0001-7273-1679

Caccıatore Ivana[6]
https://orcid.org/ 0000-0001-6253-0443

Hacımüftüoğlu Ahmet[7]
https://orcid.org/ 0000-0002-9658-3313

Çadırcı Kenan[8]
https://orcid.org/ 0000-0002-2765-4288

Stefano Antonio Di[6]
https://orcid.org/ 0000-0002-3042-2234

Mardinoğlu Adil[9,10]
https://orcid.org/ 0000-0002-4254-6090

[1]University of Bayburt, Vocational School of Health Services, Department of Medical Services and Techniques, Bayburt, Turkey [2]University of Ataturk, School of Medicine, Department of Medical Biology, Erzurum, Turkey [3]University of Sabancı, Nanotechnology Research and Application Center, İstanbul, Turkey [4]University of Erzurum Technical, Faculty of Science, Department of Molecular Biology and Genetics, Erzurum, Turkey [5]University of Ataturk, School of Medicine, Department of Medical Genetics, Erzurum, Turkey [6]University of Studies "Gabriele d'Annunzio", Department of Pharmacy, Chieti Pescara, Italy [7]University of Ataturk, School of Medicine, Department of Medical Pharmacology, Erzurum, Turkey [8]University of Health Science, Erzurum Regional Training and Research Hospital - Department of Internal Medicine [9]Science for Life Laboratory, KTH-Royal Institute of Technology, Stockholm, Sweden [10]Centre for Host-Microbiome Interactions, Faculty of Dentistry, Oral & Craniofacial Sciences, King's College London, London, United Kingdom.

Editor-in-Chief: Alexandre Rasi Aoki
Associate Editor: Fábio André dos Santos

Received: 14-Dec-2020; Accepted: 11-Sep-2021.

*Correspondence: basaktogar@bayburt.edu.tr; +90 4582111171 (T.B.).

HIGHLIGHTS

- Bioceramic nanoparticles are used to replace hard tissues.
- The toxicity of β-TCP and BCP nanoparticles is not dependent on particle size.
- BCP nanoparticles exhibit greater cytotoxic and genotoxic properties at higher concentrations as compared to β-TCP nanoparticles.
- β-TCP and BCP cause oxidative stress depending on the increase in concentration.
- Oxidative stress causes cell death and DNA damage.

Keywords: β-Tricalcium phosphate; biphasic calcium phosphate; nanoparticle; cytotoxicity; total oxidative status; genotoxicity.

GRAPHICAL ABSTRACT

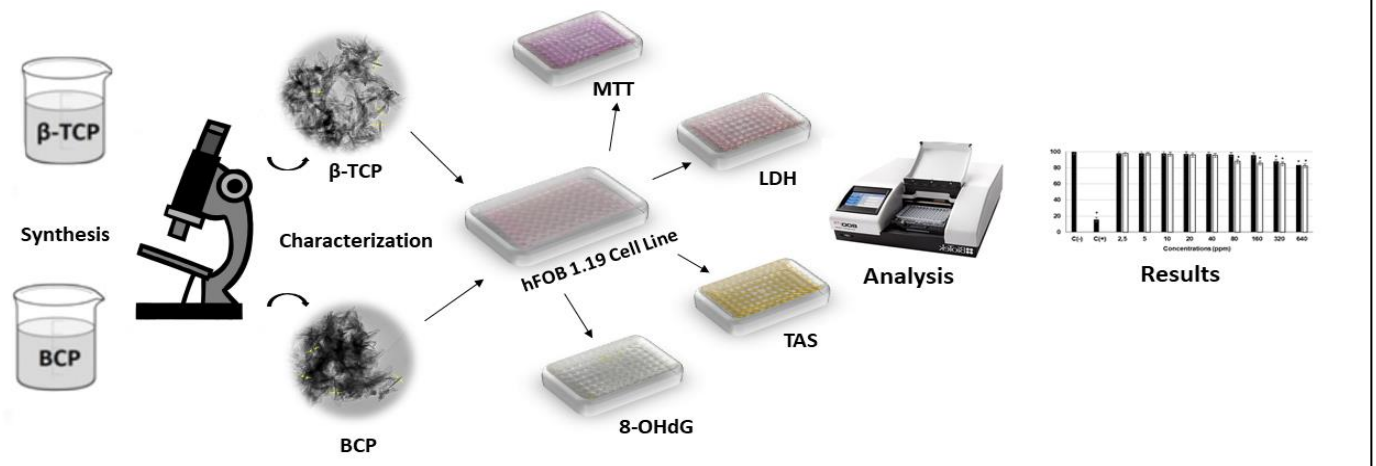

Abstract: Nanoscale biomaterials are commonly used in a wide range of biomedical applications such as bone graft substitutes, gene delivery systems, and biologically active agents. On the other hand, the cytotoxic potential of these particles hasn't yet been studied comprehensively to understand whether or not they exert any negative impact on the cellular structures. Here, we undertook the synthesis of beta-tricalcium phosphate (ß-TCP) and biphasic tricalcium phosphate (BCP) nanoparticles (NPs) and determine their concentration-dependent toxic effects in human fetal osteoblastic (hFOB 1.19) cell line. Firstly, BCP and β-TCP were synthesized using a water-based precipitation technique and characterized by X-Ray Diffraction (XRD), Raman Spectroscopy, and Transmission Electron Microscopy (TEM). The cytological effects of β-TCP and BCP at different concentrations (0–640 ppm) were evaluated by using 3- (4,5-dimethylthiazol-2-yl) -2,5-diphenyltetrazolium bromide (MTT) and lactate dehydrogenase (LDH) assays. The total oxidative status (TOS) parameter was used for investigating oxidative stress potentials of the NPs. In addition, the study assessed the DNA damage product 8-hydroxy-2′-deoxyguanosine (8-Oxo-dG) level in hFOB 1.19 cell cultures. The results indicated that the β-TCP (above 320 ppm) and BCP (above 80 ppm) NPs exhibited cytotoxicity effects on high concentrations. It was also observed that the oxidative stress increased relatively as the concentrations of NPs increased, aligning with the cytotoxicity results. However, the NPs concentrations of 160 ppm and above increased the level of 8-OH-dG. Consequently, there is a need for more systematic in vivo and in vitro approaches to the toxic effects of both nanoparticles.

INTRODUCTION

In recent years, important studies have been carried out for the development of micro and nano-scale biomaterials that mimic the physiological environment for tissue engineering researches [1]. One of these materials is bioceramics, which are widely used in orthopedics and dentistry applications [2,3]. They are commonly used for repairing or replacing the damaged hard tissues [4]. The most widely used forms of bioceramics in bone regeneration are bioactive glasses, calcium carbonates, calcium sulfates and, calcium phosphates [4]. Different compounds of synthetic calcium phosphates (CaPs) are widely used in a variety of biomedical applications owing to their excellent biocompatibility and chemical affinity towards biomolecules [5,6]. These properties make them promising biomaterials in a variety of biomedical applications [7].

Hydroxyapatite (HA), β-tricalcium phosphate (β-TCP) and, biphasic calcium phosphate (BCP, variable weight ratios of the mixtures of HA and β-TCP) are commonly used CaP compounds in the production of artificial bone cements [8,9]. Among CaPs, HA is the most stable and less soluble phase, therefore, low biodegradability of HA within the body might limit some of the applications. When compared to HA, β-TCP shows better biodegradability, thus it can be absorbed better and take over by newly generated hard tissues [10]. Since BCP contains a stable apatite phase (HA) and a more soluble/biodegradable phase (β-TCP) together, it is promising for many medical applications. As the bioactivity is directly proportional to the β-TCP/HA ratio in BCP, the bioreactivity of BCP bioceramics can be controlled by manipulating the composition and/or the crystallinity of the BCP. In chemical reactions, both BCP and β-TCP can be reconstructed from a non-stoichiometric apatite during heat treatment at above 700°C [11]. The crystal structure of non-stoichiometric apatite is similar to HA whereas, it is chemically and compositionally similar to β-TCP [10]. In vitro studies have revealed that BCP and β-TCP are biocompatible in many cell lines, such as the dog

periodontal ligament cells [12], human bone marrow stromal cells (hBMSCs) [13], human osteoblast-like cells (SaOS-2) [14], osteoblasts (SaOs-2 and MC3T3-E1 cells) [15], MC3T3-E1 osteoblast-like cells [16] and human lymphocyte cells [17]. Although nano-bioceramics-cell culture interactions have been evaluating for years, the effects of β-TCP and BCP bioceramics on the hFOB 1.19 cell line have not been investigated yet.

This study aims to evaluate the proliferative, oxidant, and genetic effects of β-TCP and BCP NPs on human fetal osteoblastic cells (hFOB 1.19) for the first time. The cytotoxic properties of β-TCP and BCP NPs were investigated by 3-(4,5-dimethylthiazol-2-yl)-2,5-diphenyltetrazolium bromide (MTT) and lactate dehydrogenase (LDH) analyses, respectively. The total oxidative status (TOS) parameter was used in assessing the biochemical effects of the particles on the hFOB 1.19 cell line. The DNA damage was also analyzed by 8-oxo-2-deoxyguanosine (8-OHdG) level as an indicator of genotoxicity.

MATERIALS AND METHODS

BCP and β-TCP synthesis

BCP and β-TCP NPs were synthesized by using a water-based precipitation technique, which was carried out according to Bakan [10]. All the compounds used in this study are analytical grade and supplied by Sigma-Aldrich® (St. Louis, MO, USA). Briefly, Ca(NO3)2.4H2O and NH4H2PO4 aqueous solutions were used as the Ca and P precursors, respectively. While the P precursor was stirred at 600 rpm, the Ca precursor was added drop by drop to the P precursor using a peristaltic pump. The reaction temperature was maintained at room temperature for synthesizing the BCP, while it was kept at 45°C for the synthesis of β-TCP. The pH was monitored during the reaction to keep it constant throughout the reaction The pH was adjusted to 8.0 and 5.5 for BCP and β-TCP, respectively. The pH was adjusted to 8.0 and 5.5 for BCP and β-TCP, respectively. After 24 h aging at room temperature, the precipitated particles were collected by filtration and were then washed with deionized water to remove NH^{4+} and NO^{3-} ions. The filter cake was then dried overnight in a vacuum oven at 80°C. Afterward, the dried powders were subsequently heated to 750°C with a heating rate of 10°C/min. The samples were held for 3h at the desired temperature followed by rapid cooling down to room temperature. The scheme of the nanoparticle synthesis procedure is shown in Figure 1.

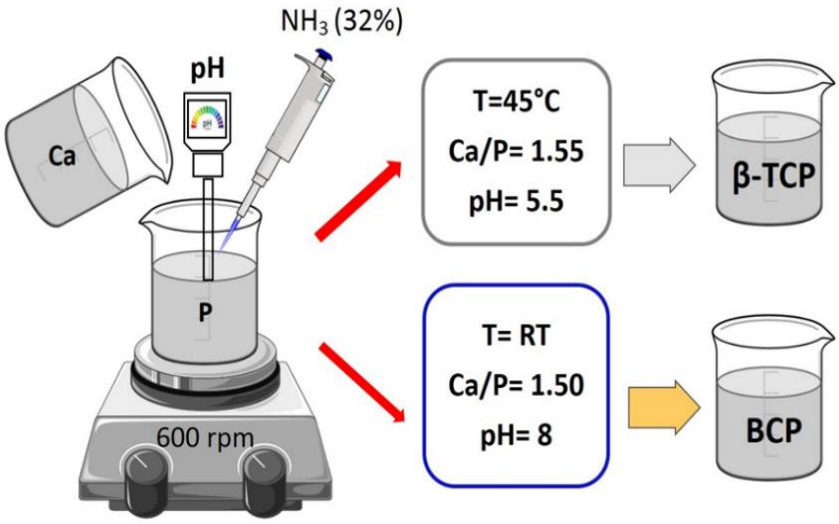

Figure 1. The scheme of the BCP and β-TCP synthesis procedures. The effect of pH and reaction temperature on the formation of β-TCP or BCP phases is revealed.

Materials characterization

X-ray diffraction (XRD) analysis was performed by a Bruker D2 Phaser for analyzing the phase composition. CuKα radiation was used at the step scanning mode, applying a tube voltage of 30 kV and a tube current of 10 mA. A step size of 0.02 and a scan speed of 1 sec/step were chosen. Also, Raman spectroscopy was used to differentiate BCP and β-TCP phases at the molecular level, even when the crystallinity degree of the samples is poor. Raman Spectroscopy measurements were carried out using a Renishaw Raman InVia System coupled with a 532 nm green laser, for identifying the characteristic (PO4)3- groups that are present in the samples. The morphology of the particles was also examined by Transmission Electron Microscopy (TEM) using a JEOL-JEM-2100F UHR7HRP TEM.

Cell Culture

Human fetal osteoblast cell line, hFOB 1.19 (CRL-11372), was purchased from American Type Cell Culture, ATCC (Manassas, USA). The hFOB 1.19 cells were cultured in Dulbecco's Modified Eagle Medium F-12, DMEM/F12 (Sigma-Aldrich®, Germany) which was supplemented with 10% fetal bovine serum (FBS) (Sigma-Aldrich®) and 1% penicillin/streptomycin (Sigma-Aldrich®). The cells were incubated in a 5% CO2 37°C humidified incubator and monitored closely for 24 hours. In this study, Triton-X-100 (1%) was used as a positive control (Control+), while the untreated cells were designed as negative control (Control−) [19-20].

MTT Cell Proliferation Assay

MTT (3- (4,5-Dimethylthiazol-2-yl) -2,5-Diphenyltetrazolium Bromide) assay kit (Cayman Chemical Company® Ann Arbor, U.S.A.) was used for cell viability and proliferation analysis. hFOB 1.19 cells were incubated at 37°C in a humidified 5% CO_2 and treated separately with BCP and β-TCP nanoparticles at different concentrations (0, 2.5, 5, 10, 20, 40, 80, 160, 320 and 640 ppm) for 72 h. 10 µL MTT solution was added to each well. The plates were incubated for 4 h at 37°C in a CO_2 incubator. DMSO solution was added to each sample, and the cultures were placed on a plate shaker with the cell containing formazan crystals. After the dissolution of all crystals using DMSO, the optical density of each sample was measured by using an ELISA reader (Bio-Tek®, USA) at 570 nm wavelength [21-22].

Lactate Dehydrogenase release (LDH) Assay

A lactate dehydrogenase cytotoxicity assay kit (Cayman Chemical Company® Ann Arbor, U.S.A.) was used for LDH analysis. After 72 hours, the cell culture was terminated and the plate was centrifuged at 400 g for 5 min. 100 µL culture medium from each well was added to a new plate. 100 µL of the reaction solution (9.6 ml of the buffer; 100X NAD+, 100X lactic acid, and 100X INT) was added to each well. The prepared plate was shaken gently with the orbital shaker for 30 min. After 30 minutes, the plate was placed in the ELISA reader to read the absorbance at 490 nm [23].

Total Oxidant Status (TOS) Assay

In this analysis, TOS (Total Oxidant Status) kit produced by Rel Assay Diagnostics® (Gaziantep, Turkey) was used. 500 µl of Reagent 1 solution was added to the wells containing 75 µl of the sample. The first absorbance at 530 nm was read. Then, 25 µl of Reagent 2 was added to the same wells and kept at room temperature for 10 min. The second absorbance at 530 nm was read [23,24]. To perform the calculation, the unit of TOS, mmol H2O2 Equiv./L, and was calculated using the following formula:

Example 2 (A2) - Example 1 (A1): A2 (Second reading) - A1 (First reading)

Result = (A2-A1)/Standard (2nd reading - 1st reading)×10µmol/L

DNA / RNA Oxidative Damage Assay

The purpose of this analysis was to determine the oxidative DNA damage in the cells by calculating the 8-OH-dG level. Therefore, DNA/RNA Oxidative Damage kit (Cayman Chemical Company® Ann Arbor, U.S.A.) was used for oxidative DNA damage assay in the culture medium. Experimental stages were carried out considering the kit procedure [25].

Statistical analysis

SPSS 22.0 software (SPSS Inc., USA) was used to carry out the statistical analysis. Results calculated as means ± SD values and the level of $p<0.05$ was accepted as statistically significant. Differences between samples were investigated using a one-way analysis of ANOVA and Duncan's test.

RESULTS

The XRD patterns of the synthesized BCP and β-TCP NPs are given in Figure 2a. Patterns were identified according to the Joint Committee on Powder Diffraction Standards (JCPDS) No:09-0432 for HA

and No: 09-0169 for β-TCP which were also given in Figure 2b. The chemical transformation of non-stoichiometric apatite to either BCP or β-TCP is revealed in the corresponding spectra.

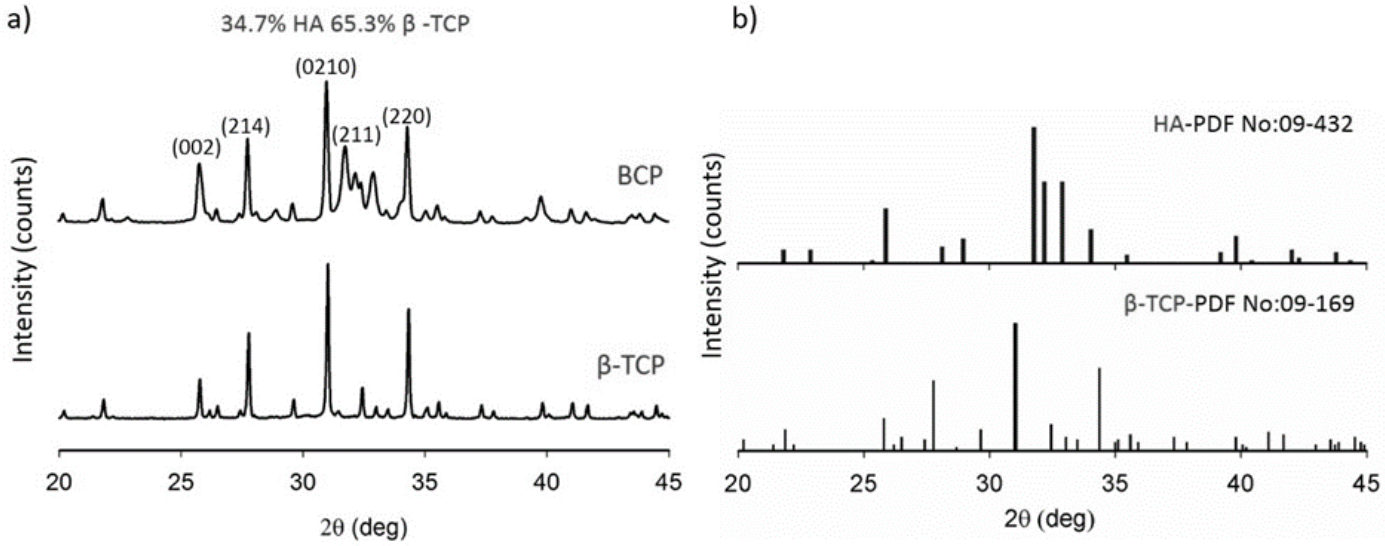

Figure 2. XRD results of the samples that were sintered at 750°C: (a) for the range of 20-45°; (b) XRD spectra of standard HA (No:09-0432) and β-TCP (No: 09-0169). The transformation from non-stoichiometric apatite to BCP or pure β-TCP was revealed.

Following the XRD analysis, Raman spectroscopy was carried out specially to confirm the formation of pure β-TCP phase. The Raman spectra of the samples are shown in Figure 3.

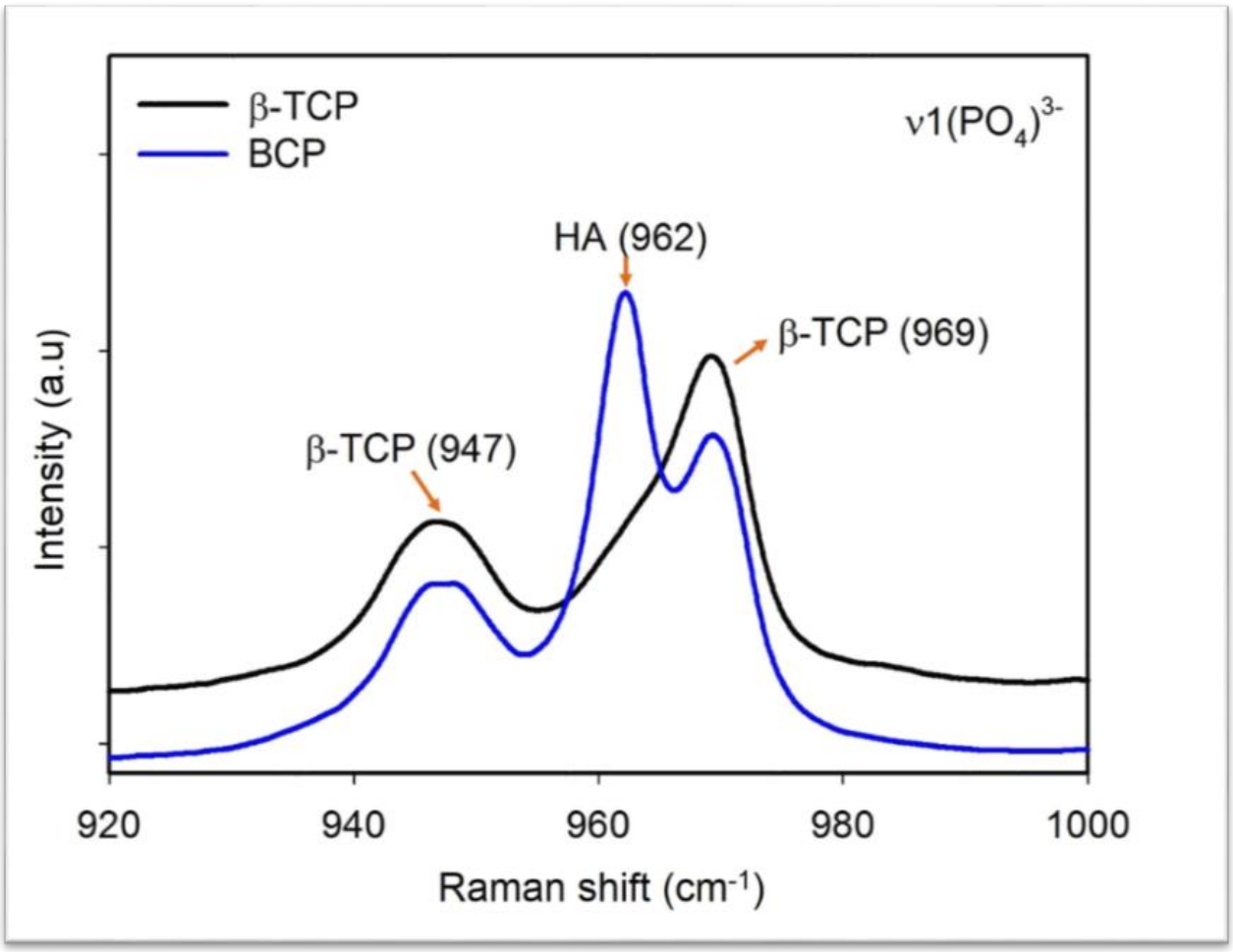

Figure 3. Raman spectra of the BCP and β-TCP samples that were sintered at 750°C. The chemical transformation of calcium-deficient hydroxyapatite to either BCP or β-TCP is revealed by tracking the most characteristic u1 (PO4)3- mode.

In Figure 4, bright-field TEM micrographs of BCP and β-TCP particles are provided. Both types of NPs are observed to be existing in rod-like morphology at the nanoscale. The diameters of both BCP and β-TCP NPs are approximately 15 nm. The lengths of the BCP particles vary from 100–150 nm while it is in the range of 75-120 nm for β-TCP NPs.

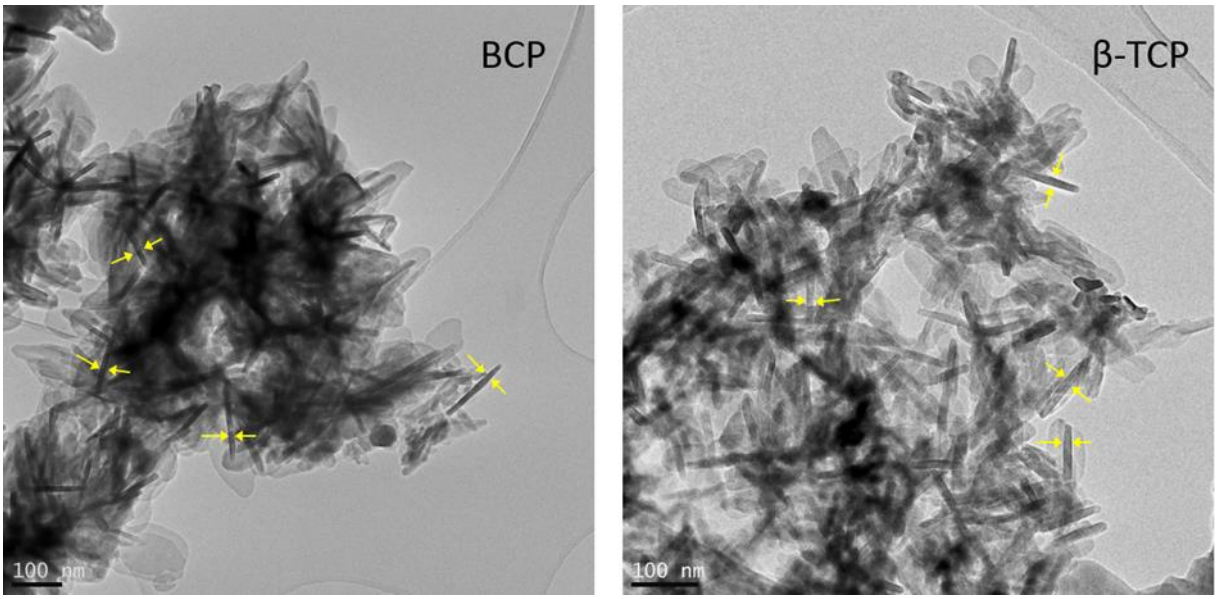

Figure 4. Bright-field TEM micrographs of BCP and β-TCP particles.

Following the structural and TEM analyses of the samples, we went onto the toxicity measurements on our samples. Cell cytotoxicity evaluation of β-TCP and BCP NPs are displayed in Figure 5. The viability of hFOB 1.19 cells treated with different concentrations of β-TCP and BCP was determined by MTT analysis after 72 hours. In the hFOB 1.19 cell line, high concentrations of BCP (except for 2.5, 5, 10, 20, and 40 ppm) decreased cell viability, while the concentrations of 320 and 640 ppm of β-TCP reduced cell viability (Figure 5.).

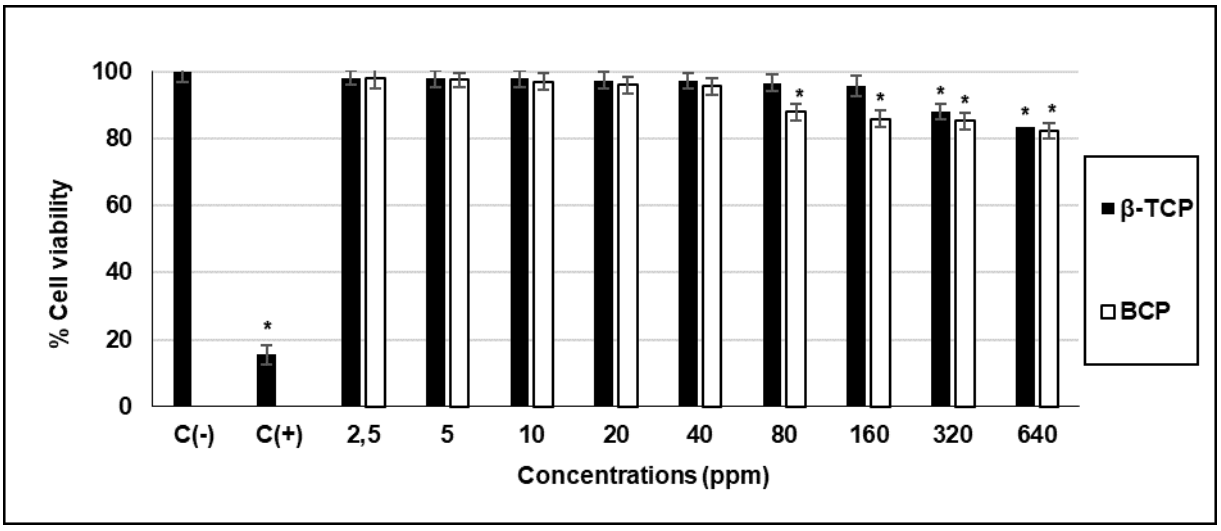

Figure 5. The *in vitro* effects of β-TCP and BCP on the cell viability of hFOB 1.19. cell line.
β-TCP: β-Tricalcium phosphate, BCP: biphasic calcium phosphate (mixtures of HA and β-TCP of varying HA/β-TCP ratios). C(-): Negative control, C(+): Positive control. *symbol presents statistical difference from C(-) group at the level of $p<0.05$. Triton-X solution was used as C(+) group.

Moreover, the cytotoxic effects of BCP and β-TCP NPs in the hFOB 1.19 cell line were determined by LDH analysis. LDH release in the hFOB 1.19 cell line put forth that only 640 ppm concentration of β-TCP increased LDH release, while the concentrations of 40, 80, 160, 320, 640 ppm of BCP significantly increased LDH release compared with the control group ($p<0.05$). All results are shown in Figure 6.

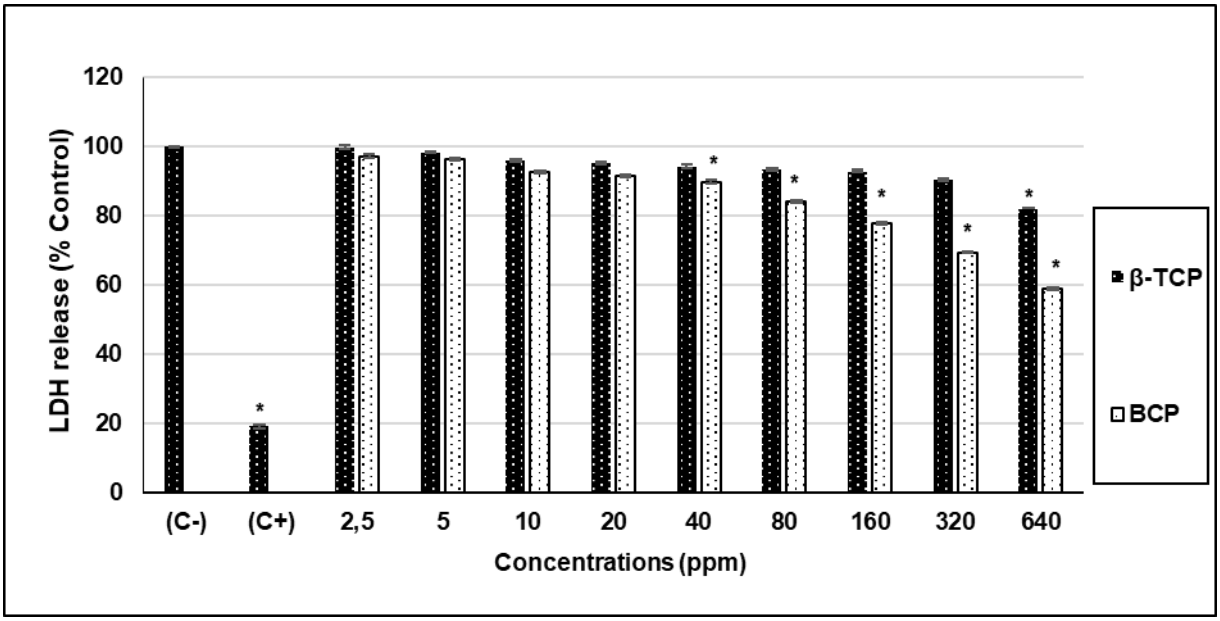

Figure 6. Cytotoxic effects of β-TCP and BCP in hFOB 1.19. cell line. Abbreviations are the same as denoted in Figure 5.

In order to evaluate the overall oxidation state, TOS analysis was also performed for 72 hours after application of different concentrations of β-TCP and BCP (2.5, 5, 10, 20, 40, 80, 160, 320, and 640 ppm) to determine the total oxidant status on hFOB 1.19 cell line. When the TOS levels of biomaterials on hFOB cell line were examined, it was determined that high concentrations of β-TCP and BCP NPs caused low oxidative stress (Table 1).

Table 1. TOS levels generated by β-TCP and BCP tested on hFOB 1.19. cells.

hFOB 1.19. cell line		
TOS level (as H_2O_2 equiv./μmol L^{-1})		
Concentrations (as ppm)	**β-TCP**	**BCP**
Control-	1.9 ± 0.15	1.9 ± 0.15
Control+	8.1 ± 0.59*	8.1 ± 0.59*
2.5	1.8 ± 0.21	1.6 ± 0.21
5	1.6 ± 0.32	1.8 ± 0.39
10	1.8 ± 0.27	1.9 ± 0.36
20	1.9 ± 0.38	2.1 ± 0.26
40	2.0 ± 0.21	2.3 ± 0.23
80	2.1 ± 0.23	2.5 ± 0.27*
160	2.2 ± 0.32	2.8 ± 0.28*
320	2.9 ± 0.23*	3.1 ± 0.31*
640	3.1 ± 0.32*	3.3 ± 0.36*

At 72 hours after administration of β-TCP and BCP, 8-OH-dG levels were measured in cells to determine oxidative DNA damage levels on hFOB 1.19 cells. Based on 8-OH-dG levels on hFOB cells, it was revealed that the concentrations of 320 and 640 ppm of β-TCP and the concentrations of 80, 160, 320 and 640 ppm of BCP created weakly DNA damage compared to the control group ($p<0.05$, Table 2.).

Table 2. 8-OH-dG level observed in hFOB 1.19. cells treated with β-TCP and BCP

hFOB 1.19. cell cultures		
8-OH-dG level (pmol/µg)		
Concentrations (as ppm)	**β-TCP**	**BCP**
Control-	0.7 ± 0.15	0.7 ±0.15
Control+	3.6 ± 0.17*	3.6 ± 0.14*
2.5	0.6 ± 0.18	0.7 ± 0.14
5	0.8 ± 0.16	0.7 ± 0.11
10	0.7 ± 0.20	0.8 ± 0.16
20	0.8 ± 0.18	0.9 ± 0.14
40	0.9 ± 0.16	1.0 ± 0.13
80	0.9 ± 0.19	0.9 ± 0.15
160	1.0 ± 0.14	1.4 ± 0.18*
320	1.1 ± 0.17*	1.8 ± 0.13*
640	1.8 ± 0.19*	2.3 ± 0.15*

DISCUSSION

One of the most important advances in biomaterial science is the development of bioceramic nanoparticles (NPs), which can be utilized for the replacement of hard tissues [26]. On the other hand, engineered NP's, whose toxic effects are not fully known, can be dangerous for human health. [27]. Therefore, it is required to apply current toxicity protocols to determine the toxic effects of NPs [28,29]. In this study, to understand the possible damages that may be caused by nano-biomaterials, we investigated the potential nanotoxicity of β-tricalcium phosphate (β-TCP) and biphasic calcium phosphate (BCP) NPs on human fetal osteoblastic (hFOB 1.19) cell line. In our study, firstly, β-TCP and BCP NPs were synthesized using a water-based precipitation technique and were then characterized. The XRD results and Raman spectroscopy confirm the formation of BCP and β-TCP phases as desired during the synthesis. As can be seen from the XRD patterns, the pure β-TCP phase could be obtained by adjusting the synthesis parameters to those prescribed in the methods section. Raman method was chosen as a complementary method to back the XRD results as the former is rather sensitive to variations in fine structure in specific cases such as in this work. As BCP consists of HA and β-TCP phases, Raman spectroscopy can provide a better estimation of the chemical transformation of non-stoichiometric apatite to either β-TCP or BCP [10]. The difference between the number of (PO4)3- groups in the unit cells of HA and β-TCP causes different Raman scattering aiding in distinct identification of the two phases. Both HA and β-TCP are dominated by the internal (PO4)3- modes and, therefore, the Raman spectra of the samples were evaluated particularly considering the most characteristic υ1 (PO4)3- mode. The band at 962 cm-1 is assigned to the totally symmetric stretching mode (υ1) of the tetrahedral (PO4)3- group which corresponds to the HA phase. The same vibration mode can be observed at 969 cm^{-1} accompanied by a wide band at 940-950 cm^{-1} in the β-TCP spectrum [30,31]. As toxicity can depend on the morphology of the particles, we carried out a transmission electron microscopy (TEM) analysis of the samples. The TEM results reveal highly identical morphologies for both sample types despite their compositional and synthesis method differences. That the two samples, albeit different in chemistry and synthesis conditions, display identical morphologies helped us to eliminate the morphology as a major parameter on the toxicity effects.

In our study, MTT method was used to determine the viability of cells exposed to β-TCP and BCP NPs in hFOB 1.19 cell culture while LDH method was used to determine cytotoxicity. Our MTT results showed that both β-TCP (above 320 ppm) and BCP (above 80 ppm) nanoparticles caused a decrease in cell viability depending on the increasing concentration (Fig. 5, $p< 0.05$). Likewise, the LDH results indicated that the β-TCP (640 ppm) and BCP (above 40 ppm) NPs exhibited cytotoxicity effects on high concentrations, rendering both NPs are non-toxic below these concentrations (Fig. 6, $p< 0.05$). The obtained results showed that the LDH release test is supportive of the MTT test. Similar to our results, Mitri and coauthors [32] investigated the cytotoxic effects of BCP and HA using the Neutral Red test on the human mesenchymal cell line. They reported that HA and BCP extracts induced slight cytotoxicity, with cell survival under 75% of control. In a recent study, the proliferative effects of β-TCP on MG-63 cell line using the MTT analysis and time-dependence cytotoxicity on MG-63 cells were reported Bakan [10]. On the other hand, Abdullah and coauthors [33] combined zirconia, and β-TCP with polyamide 12 in their studies. They used human periodontal ligament fibroblast cells to assess the cytotoxicity of the materials by the MTT assay. As a result, they found polyamide filled with hybrid ceramics (zirconia and β-TCP) increased the cell viability compared

to the empty polyamide. Besides, Chen and coauthors [34] revealed that HA, BCP and β-TCP could promote proliferation of human umbilical vein endothelial cells (HUVECs).

One of the in vitro toxicity assessments is to examine the total state of oxidant molecules in the serum [23,24]. In this work, the toxic effects of β-TCP and BCP on hFOB 1.19 cell and whether these effects are oxidative stress-induced were investigated. In the study, BCP increased the TOS value statistically at 80 ppm and above concentrations, while β-TCP caused an increase in TOS value at 320 and 640 ppm concentrations (Table 1, $p<0.05$). Liu and coauthors [35] reported that 400 mg/kg β-TCP caused an increase in Ca2+ and PO43- ions as a result of intracellular degradation. They also reported that 400 mg/kg β-TCP caused an increase in reactive oxygen species (ROS) in HepG2 cells in their study. Our findings are similar to be to that reported by Liu and colleagues. In both studies, the increase in concentration caused an increase in ROS production. This situation triggered oxidative stress. According to TOS levels, oxidative stress may be one of the most important mechanisms by which β-TCP and BCP NPs exhibit cytotoxic effects. In addition to, oxidative modifications are one of the most important causes of cellular DNA damage [36,37]. In our current study, to test DNA oxidative damage, we assayed 8-OHdG levels by ELISA. Results indicated that the levels of 8-OHdG increased differently in the biomaterials-exposure groups compared to the control group, as shown in Table 3. ($p<0.05$). When levels of oxidative DNA damage occurred by tested biomaterials on hFOB1.19 cell were examined, it was revealed that BCP-induced genotoxicity was higher and statistically different than β-TCP. Contrary to our 8-OHdG results, in a single study on the genotoxic effects of BCP, single-cell gel electrophoresis (Comet) assay was used. It was proven that the BCP of modified porosity did not exhibit any genotoxic effect on human dental pulp cells (HDPCs) [38]. Furthermore, Akbaba and Turkez [17] revealed that β-TCP did not show genotoxic effects on human peripheral blood cultures in vitro, even at the highest concentrations.

CONCLUSION

In the present study, the biochemical effects, cytotoxicity, and genotoxicity potentials of β-TCP and BCP on hFOB 1.19 cell line were evaluated by using MTT, LDH, TOS and DNA-RNA damage methods. Our findings exhibited that cytotoxicity of the particles was found to be strongly dependent on concentration. As the TEM analysis revealed that the morphologies of the two samples are identical, we rule out the morphology as a major cause in the differences among the toxicity-related tests. It was found that there were thresholds for each particle's toxicity and the safety of the particles was related to these specific concentration intervals. When these thresholds were exceeded, oxidative stress and DNA damage occurred in cell culture. This study has revealed that safety reports must be prepared according to tissue types and concentration that the nanoparticles were applied.

Acknowledgments: Dr. Umut Savacı and Prof. Dr. Servet Turan are gratefully acknowledged for providing technical support for TEM analysis.
Conflict interest: The author(s) declared no potential conflicts of interest concerning the research, authorship, and/or publication of this article.

REFERENCES

1. Skoog SA, Kumar G, Narayan RJ, Goering PL. Biological responses to immobilized microscale and nanoscale surface topographies. Pharmacol Ther. 2018;182:33-55.
2. Sanz JL, Lozano FJR, Llena C, Sauro S, Forner L. Bioactivity of Bioceramic Materials Used in the Dentin-Pulp Complex Therapy: A Systematic Review. Materials (Basel) 2019;12(7).
3. Nabiyouni M, Brückner T, Zhou H, Gbureck U, Bhaduri SB. Magnesium-based bioceramics in orthopedic applications. Acta Biomater. 2018;66:23-43
4. Mala R, Ruby Celsia AS. Bioceramics in orthopaedics: A review. Fundamental Biomaterials: Ceramics. 2018:195-221.
5. Masouleh MP, Hosseini V, Pourhaghgouy M, Bakht MK. Calcium Phosphate Nanoparticles Cytocompatibility Versus Cytotoxicity: A Serendipitous Paradox. Curr Pharm Des. 2017;23(20):2930-51.
6. Hurle K, Neubauer J, Goetz-Neunhoeffer F. Hydration mechanism of partially amorphized β-tricalcium phosphate. Acta Biomater. 2017; 54:429-40.
7. Epple M. Review of potential health risks associated with nanoscopic calcium phosphate. Epple M. Acta Biomater. 2018;77:1-14.
8. Sánchez-Salcedo S, Nieto A, Vallet-Regi M. Hydroxyapatite/β-tricalcium phosphate/agarose macroporous scaffolds for bone tissue engineering. Chem Eng J. 2008;137:62-71.
9. Xidaki D, Agrafioti P, Diomatari D, Kaminari A, Tsalavoutas-Psarras E, Alexiou P, et al. Synthesis of hydroxyapatite, β-tricalcium phosphate and biphasic calcium phosphate particles to act as local delivery carriers of curcumin: loading, release and in vitro studies. Materials. 2018;11(4):595-607.

10. Bakan F. Systematic Study of the Effect of pH on the Initialization of Ca-deficient Hydroxyapatite to β-TCP Nanoparticles. Materials. 2019:12(3);354.
11. Dorozhkina E, Dorotzhkin S. Mechanism of the solid-state transformation of calcium-deficient hydroxyapatite (CDHA) into biphasic calcium phosphate (BCP) at elevated temperatures. Chem Mater. 2002;14:4267-72.
12. Liu G, Zhao L, Cui L, Liu W, Cao Y. Tissue-engineered bone formation using human bone marrow stromal cells and novel beta-tricalcium phosphate. Biomed Mater. 2007;2:78-86.
13. Zhong JS, Ouyang XY, Mei F, Deng XL, Cao CF. Construction of 3D complex of porous beta-tricalcium phosphate/collagen scaffolds and dog periodontal ligament cells. Beijing Da Xue Xue Bao Yi Xue Ban. 2007;39(5):507-10.
14. Wang S, Wang X, Draenert FG, Albert O, Schröder HC, Mailänder V, et al. Bioactive and biodegradable silica biomaterial for bone regeneration. Bone. 2014;67:292-304.
15. Arbez B, Libouban H. Behavior of macrophage and osteoblast cell lines in contact with the β-TCP biomaterial (beta- tricalcium phosphate). Morphologie. 2017;101(334):154-63.
16. Taz M, Bae SH, Jung HI, Cho HD, Lee BT. Bone regeneration strategy by different sized multichanneled biphasic calcium phosphate granules: In vivo evaluation in rabbit model. J Biomater Appl. 2018;32(10):1406-20.
17. Akbaba GB, Türkez H. Investigation of the genotoxicity of aluminum oxide, β-tricalcium phosphate, and zinc oxide nanoparticles *ın vitro*. Int J Toxicol. 2018;37(3):216-22.
18. Bakan, F. Gene delivery by hydroxyapatite and calcium phosphate nanoparticles: a review of novel and recent applications. Hydroxyapatite-Advances in Composite Nanomaterials, Biomedical Applications and Its Technological Facets. 2018;157-76.
19. Hapidin H, Romli NAA, Abdullah H. Proliferation study and microscopy evaluation on the effects of tannic acid in human fetal osteoblast cell line (hFOB 1.19). Microsc Res Tech. 2019;82(11):1928-40.
20. Abdullah AR, Hapidin H, Abdullah H. The Role of Semipurified Fractions Isolated from Quercus infectoria on Bone Metabolism by Using hFOB 1.19 Human Fetal Osteoblast Cell Model. Evid Based Complement Alternat Med. 2018;5319528.
21. Türkez H, Arslan ME, Sönmez E, Tatar A, Açikyildiz M, Geyikoğlu F. Toxicogenomic responses of human alveolar epithelial cells to tungsten boride nanoparticles. Chem. Biol. Int. 2017;273:257–65.
22. Togar B, Celik K, Turkez H. In vitro Cytotoxic, Genotoxic and Antioxidant/Oxidant Effects of Guaiazulene on Human Lymphocytes. Braz. Arch. Biol. Technol. 2015;58(1):61-7.
23. Türkez H, Arslan ME, Sönmez E, Geyikoğlu F, Açıkyıldız M, Tatar A. Microarray assisted toxicological investigations of boron carbide nanoparticles on human primary alveolar epithelial cells. Chem Biol Int. 2019;300:131-7.
24. Emsen B, Guven B. Activities of two edible macrofungi, *Coprinus comatus* and *Leucoagaricus leucothites* in human lymphocytes: cytogenetic and biochemical study. Plant Biosystems. 2019:362-8.
25. Emsen B, Aslan A, Turkez H, Joughi A, Kaya A. The anti-cancer efficacies of diffractaic, lobaric, and usnic acid: In vitro inhibition of glioma. J Cancer Res Ther. 2018:14(5);941-9.
26. Morejón L, Delgado JA, Antunes Ribeiro A, Varella de Oliveira M, Mendizábal E, García I, et al. Development, Characterization and in vitro biological properties of scaffolds fabricated from calcium phosphate nanoparticles. Int J Mol Sci. 2019;11:20.
27. Khan HA, Shanker R. Toxicity of Nanomaterials. Biomed Res Int. 2015;2015:521014.
28. Ghaffari R, Salimi-Kenari H, Fahimipour F, Rabiee SM, Adeli H, Dashtimoghadam E. Fabrication and characterization of dextran/nanocrystalline beta-tricalcium phosphate nanocomposite hydrogel scaffolds. Int J Biol Macromol. 2020;148:434-48.
29. Cusco R, Guitian F, de Aza S, Artus L. Differentiation between hydroxyapatite and β-tricalcium phosphate by means of μ-raman spectroscopy. J Eur Ceram Soc. 1998;18:1301–05.
30. Ratner BD. The biocompatibility manifesto: biocompatibility for the twenty-first century. J Cardiovasc Transl Res. 2011;4(5):523-7.
31. Ebrahimi M, Botelho MG, Dorozhkin SV. Biphasic calcium phosphates bioceramics (HA/TCP): Concept, physicochemical properties and the impact of standardization of study protocols in biomaterials research. Mater Sci Eng C Mater Biol Appl. 2017;71:1293-1312.29.
32. Mitri F, Alves G, Fernandes G, König B, Rossi AJ, Granjeiro J. Cytocompatibility of porous biphasic calcium phosphate granules with human mesenchymal cells by a multiparametric assay. Artif Organs. 2012;36(6):535-42.
33. Abdullah AM, Rahim TNAT, Hamad WNFW, Mohamad D, Akil HM, Rajion ZA. Mechanical and cytotoxicity properties of hybrid ceramics filled polyamide 12 filament feedstock for craniofacial bone reconstruction via fused deposition modelling. Dent Mater. 2018;34(11):e309-16.
34. Chen Y, Wang J, Zhu XD, Tang ZR, Yang X, Tan YF, Fan YJ, Zhang XD. Enhanced effect of β-tricalcium phosphate phase on neovascularization of porous calcium phosphate ceramics: *in vitro* and in vivo evidence. Acta Biomater. 2015;11:435-48.
35. Liu L, Dai H, Wu Y, Li B, Yi J, Xu C, et al. In vitro and in vivo mechanism of hepatocellular carcinoma inhibition by beta-TCP nanoparticles. Int J Nanomedicine. 2019;14:3491-502.
36. Geyikoglu F, Türkez H. Protective effect of sodium selenite on genotoxicity to human whole blood cultures induced by aflatoxin B1. Braz Arch Biol Technol. 2005;48(6):905–10.

37. Kulkarni Aranya A, Pushalkar S, Zhao M, LeGeros RZ, Zhang Y, Saxena D. Antibacterial and bioactive coatings on titanium implant surfaces. J. Biomed. Mater. Res. - Part A. 2017;105(8):2218–27.
38. Wahab NFAC, Kannan TP, Mahmood Z, Rahman IA, Ismail H. Genotoxicity assessment of biphasic calcium phosphate of modified porosity on human dental pulp cells using Ames and Comet assays. Toxicol in vitro. 2018;47:207–12.